# Gas-Phase Reactivity of the $Ti_8C_{12}^+$ Met-car with Triatomic Sulfur-Containing Molecules: $CS_2$, SCO, and $SO_2$

**James M. Lightstone,† Melissa J. Patterson,† Ping Liu,‡ and Michael G. White*,†,‡**

*Department of Chemistry, SUNY Stony Brook, Stony Brook, New York 11794, and Chemistry Department, Brookhaven National Laboratory, Upton, New York 11973*

*Received: December 13, 2005; In Final Form: January 17, 2006*

Gas-phase $Ti_xC_y^+$ clusters ($x/y$ = 3/5, 4/7, 5/9, 6/9, 7/12, 8/12, 9/12) including the magic $Ti_8C_{12}^+$ (met-car) have been produced by reactive sputtering with a magnetron cluster source. The gas-phase reactivity of the met-car with SCO, $CS_2$, and $SO_2$ was investigated in a hexapole collision cell by way of tandem mass spectrometry. Results indicate an increase in activity as the oxygen-to-sulfur ratio increases ($SO_2$ > SCO > $CS_2$) with products ranging from association to break down of the met-car cluster. Trends in the mass spectra also indicate SCO and $CS_2$ may bond to the met-car in a unique way not observed in previous reactivity studies on $Ti_8C_{12}^+$. To investigate this, several possible single molecule−cluster bonding configurations were calculated with density functional theory. The results indicate that bridge bonding of the intact molecules is energetically preferred. In addition, the energy barriers and transition states leading to dissociation products were calculated and the trends are found to be in qualitative agreement with experiment. The effects of the different types of bonding and number of adsorbed species on the reactivity of the met-car along with proposed reaction mechanisms for product formation are also discussed.

## I. Introduction

Since its discovery by Castleman and co-workers,[1−4] the $Ti_8C_{12}$ metallocarbohedrene (met-car) cluster has been extensively studied for its unique cage-like structure, stability, photochemistry, and reactivity with a wide variety of molecular adducts.[5,6] Theoretical modeling of the structure shows that the eight Ti atoms are all exposed at "edge" sites, with two sets of four chemically equivalent Ti atoms arranged in inner and outer near-tetrahedra (overall $D_{2d}$ or $C_1$ symmetry).[7−12] Polar molecules such as $H_2O$, $NH_3$, and $CH_3OH$ form adducts with up to eight molecules, confirming the number of exposed metal sites.[13−16] Larger $\pi$-conjugating systems such as benzene form adducts with a maximum of four "adsorbed" molecules, presumably $\eta-\pi$ bonded at the outer Ti sites.[8,14−16] Recent DFT calculations have shown that the local electron density around the Ti atoms is strongly influenced by the bridging $C_2^-$ units that can be considered as "reservoirs" of negative charge.[9,10] This property allows the Ti atoms to act as Lewis acids when interacting with nucleophilic systems (e.g., $H_2O$, $NH_3$, $C_6H_6$) or to be oxidized by strongly electron withdrawing groups (e.g., Cl, I).

Gas-phase metallocarbohedrene species can also be viewed as nanostructured forms of the early transition metal carbides (e.g., TiC, MoC/$Mo_2C$, WC), which in their bulk form have attracted considerable interest as dehydrogenation, isomerization, and desulfurization catalysts.[17,18] The early transition metals (e.g., Ti, Mo, W) are very active, but nonselective catalysts, alloying with carbon results in carbidic surfaces whose catalytic performance is characteristic of the Group 10 noble metals, Pt and Pd.[17−21] Surface science studies have also shown that the reactivity of metal carbide surfaces depends on the degree of carburization, with certain reactions being poisoned by high carbon coverages.[22−24]

The effect of the C:Ti ratio on activity was investigated in a series of recent papers by Liu and co-workers using DFT in which they compared the reactivity of the $Ti_8C_{12}$ met-car and $Ti_{14}C_{13}$ nanocrystallite with extended surfaces of the corresponding bulk metal carbide.[9,25] The calculated binding energies for CO, $NH_3$, and $H_2O$ were found to be highest for the $Ti_8C_{12}$ met-car compared to the $Ti_{14}C_{13}$ nanocrystallite and the TiC(001) single-crystal surface, despite having the highest C:Ti ratio.[9] The calculated binding energies for $SO_2$ showed a similar trend to that found for CO, $NH_3$, and $H_2O$.[25] Moreover, the calculations show that complete dissociation of $SO_2$ is energetically favorable on the $Ti_8C_{12}$ met-car, with the O-atoms bridge-bonded across an outer Ti−C bond and the S-atom bonded to the adjacent inner Ti-atom. The dissociation of $SO_2$ on the met-car can be contrasted to the weak molecular binding of $SO_2$ on the TiC(001) single-crystal surface.[25] These theoretical studies highlight the fact that carbon plays an essential role determining the activity of the exposed metal sites (ligand effect) and is not simply a spectator or site blocker. In addition, the calculations suggest the $Ti_8C_{12}$ met-car may be active toward decomposition of sulfur-containing molecules.

As a follow up to the theoretical work discussed above, we present the first gas-phase reactivity studies of the $Ti_8C_{12}^+$ met-car cation with sulfur-containing compounds $CS_2$, SCO, and $SO_2$. The triatomic molecules were chosen in order to study reactivity as a function of varying sulfur content. These experiments were performed in a cluster ion beam apparatus that uses reactive sputtering in a magnetron source for generating cation clusters. The latter are mass selected and then passed through a high-pressure collision cell for studies of adduct formation or reaction. Product ions exiting the collision cell were mass analyzed by a second quadrupole filter. Assignments of the reaction product mass spectra were assisted through the use

* Address correspondence to this author.
† State University of New York at Stony Brook.
‡ Brookhaven National Laboratory.

10.1021/jp057277b CCC: $33.50 
Published on Web 02/14/2006

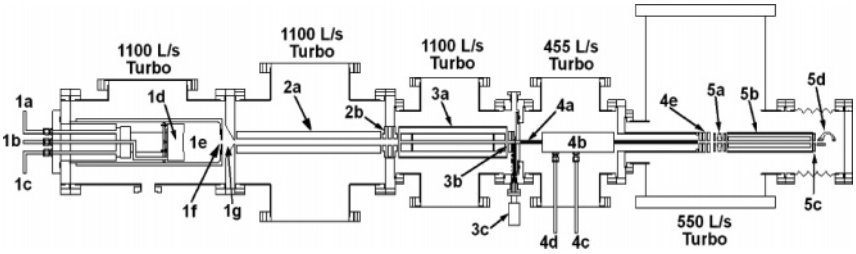


**Figure 1.** Schematic of the experimental apparatus: (1a) aggregation gas inlet, (1b) discharge gas inlet, (1c) baratron, (1d) magnetron, (1e) aggregation tube, (1f) apertures, (1g) differential pumping region; (2a) quadrupole ion guide, (2b) lenses; (3a) mass selecting quadrupole, (3b) lens gate-valve, (3c) linear drive for gate-valve isolation; (4a) hexapole ion guide, (4b) collision cell, (4c) reactive gas inlet, (4d) baratron, (4e) lenses; (5a) lenses, (5b) quadrupole mass selector, (5c) lens, (d) channeltron.

of isotopically labeled sulfur compounds ($C$,[13] $O$,[18] $S$[34]), and $C^{13}H_4$ which could be used to generate the isotopically labeled $Ti_8C_{12}$[(13)] met-car cluster. This approach is similar to that employed in previous reactivity studies on metallocarbohedrene cation clusters.[13,14,26,27] The sulfur molecules studied here exhibit increasing activity as the oxygen-to-sulfur ratio increases. Significant reaction products are observed with the triatomic molecules $CS_2$, SCO, and $SO_2$, ranging from simple adduct formation to breakdown of the $Ti_8C_{12}^+$ cluster.

## II. Experimental Section

The work presented here was performed on a newly constructed cluster beam apparatus designed for the study of cluster ion reactivity in the gas phase and deposited on surfaces. A diagram of the instrument, illustrated in Figure 1, shows the individual components housed in five independently pumped, stainless steel chambers (sections 1−5). This arrangement maximizes the differential pumping needed to isolate the high-pressure magnetron ion source (a few Torr) from the UHV environment of the final vacuum chamber ($1-5 \times 10^{-9}$ Torr). Differential pumping is achieved by small beam apertures placed between sections 1−5 and the use of high-speed turbomolecular pumps (1100 L/s; Osaka Vacuum) in the first three stages. The main components of the instrument are a magnetron sputtering ion source (section 1), a differential pumping section containing a quadrupole ion guide (section 2), a quadrupole mass filter for mass selection of the clusters (section 3), a hexapole ion guide that includes an enclosed section for collisional studies with gas-phase molecules (section 4), and a second quadrupole mass filter (section 5) for detection of ion products generated in the collision cell. Electrostatic lens elements (2b, 3b, 4e and 5a, Figure 4) are used to transmit the cluster ions between the ion guides and quadrupole mass filters. A small gate valve (3c, Figure 4) can be used to separate the final two chambers for servicing the source region while maintaining UHV conditions in the final stages of the beam line. More detailed descriptions of the individual components are given below.

**Cluster Source.** Cluster ions are produced by a magnetron sputtering ion source (1d; Oxford Scientific) mounted in a cylindrical tube that defines the high-pressure region for cluster formation (1e). The surrounding tube can also be cryogenically cooled, which for some materials enhances cluster growth. Cooling the shield did not improve the production of the $Ti_8C_{12}^+$ met-car cluster, and it was used at room temperature for the studies reported here. A gas mixture containing ∼2% methane in argon was used for sputtering the Ti target and creating carbon species in the plasma for reaction. Clusters are formed via collisions with He (aggregation) gas that are added to the source and controlled independently of the sputtering gas. The distance between the magnetron head and the exit aperture of the surrounding shield (4 mm diameter; 1f) can be varied and is used for optimizing the cluster mass range of interest. The cluster beam emerging from the source passes into a differential pumping region (1g) where it is collimated by a second aperture (5 mm diameter) before entering the first ion guide (2a).

Optimal production of the $Ti_8C_{12}^+$ met-car occurred with a sputtering power of 220 W (at 1.15 amps), a total source pressure of 5−6 Torr ($Ar/CH_4$ + He), and an aggregation distance of ∼3 cm (1e). Typical operating pressure in the differential-pumping region just beyond the source exit aperture was $10^{-2}-10^{-3}$ Torr (1g). These operating conditions define a narrow window for the production of the $Ti_8C_{12}^+$ cluster, such that small variations in parameters lead to a decrease in the met-car intensity and an increased yield of other $Ti_xC_y^+$ clusters.

**Ion Guide.** The first quadrupole ion guide (2a) is constructed from 19 mm stainless steel rods with a center diameter of 1.6 cm. The high-voltage radio frequency (RF) driving field is provided by a custom built power supply based on the design by Jones et al.[28] The supply provides two RF signals 180° out of phase at a frequency of ∼880 kHz and a peak-to-peak amplitude controlled by an external high-voltage power supply (Bertan High Voltage). The RF amplitude is typically around 600 V, as determined by maximizing the $Ti_8C_{12}^+$ signal.

**Mass Selector.** Mass selection of the cluster ions is achieved via a quadrupole mass filter, using 19 mm rods (21 cm long) retrofitted with pre- and postfilters (3a). The filters are 3.8 cm long extensions mounted on both ends of the quadrupole rods and are electrically isolated via an insulating collar. The filters are inductively coupled to the RF from the main rod system. Such an arrangement has been found to decrease fringing fields around the quadrupole entrance and exit apertures, thus helping to increase ion throughput.[29] The filters can also be used as lens elements by applying a small DC voltage that is isolated from the RF potential via high-voltage blocking resistors. The entire rod system is mounted inside a stainless steel canister that is held at ground potential. The RF high voltage is provided by a custom built power supply operating at a frequency of 292 kHz (Extranuclear). At this relatively low operating frequency, the quadruple filter can reach masses as high as 10 000 amu.

**Hexapole Ion Guide and Collision Cell.** The hexapole ion guide (4a) is constructed from six 2.3 mm diameter stainless steel rods, 44.9 cm in length, held in place by four ceramic mounts (ABB Extrel). The ion guide is driven by a custom RF power supply operating at a frequency of 660 kHz with a peak-to-peak amplitude of 20−40 V. A stainless steel gas collision cell with a 4.1 cm inner diameter and 18.1 cm in length is mounted around two of the ceramic insulators holding the rods, the first of which is located 5.3 cm from the entrance of the ion guide (see 4b). Stainless steel end caps fit with Teflon apertures further support the rods and reduce the diameter of the entrance and exit openings to 0.7 cm. Reactive gases are introduced into

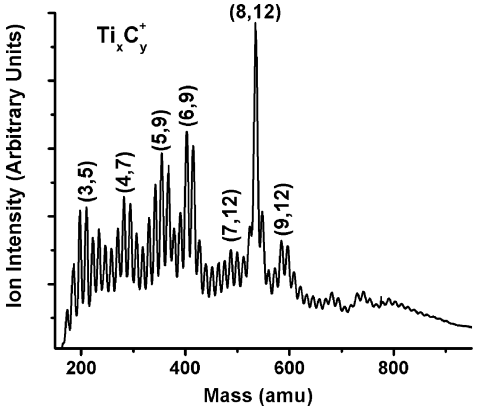


**Figure 2.** Mass spectrum of the $Ti_xC_y^+$ clusters produced by a magnetron cluster source. The apparent sudden onset of signal at 200 amu is only an artifact of our quadrupole power supply and not a true representation of the cluster distribution produced by the cluster source.

the center of the collision cell (4c) with a variable leak valve (Varian Vacuum). A second port (4d) mounted opposite to the first is used to monitor the pressure inside the collision cell with a capacitance manometer (MKS). Typical pressures measured in the gas cell are 8−10 mTorr with a background pressure in the surrounding vacuum chamber of $5-10 \times 10^{-5}$ Torr. Ion products generated by cluster−gas collisions exit the gas cell and are transported by the hexapole ion guide to a lens stack (4e) that focuses the ions onto the entrance aperture of the analyzing mass spectrometer (5a−d).

**Product Detection.** Ions exiting from the hexapole ion guide are mass analyzed by a quadrupole mass spectrometer with 9.5 mm diameter rods and operating at 880 kHz (ABB EXTREL). The mass filtered ions are detected by a combination of accelerating dynode and channel electron multiplier (Burle) biased at −4.0 and −1.89 KV, respectively. The current from the channeltron is read by a digital picoammeter (Keithly Instruments) and the signal recorded by a PC with an analog to digital converter (National Instruments) and data acquisition software (Labview).

## III. Results and Discussion

Figure 2 shows a mass spectrum of the $Ti_xC_y^+$ cation clusters produced by the magnetron source. A wide range of metal-to-carbon stoichiometries are observed in the range 200−900 amu, e.g., $(x, y) = (3, 5), (4, 7), (5, 9), (6, 9), (7, 12), (8, 12)$, and (9, 12), beyond which it becomes difficult to discern individual peaks above the background signal. The intense peak at 528 amu is the correct mass for the $Ti_8C_{12}^+$ met-car cluster first discovered by Castleman et al.[1] To confirm this assignment, methane enriched with carbon-13 was substituted in the sputtering gas mixture and the resulting mass spectrum was compared to that from carbon-12. A mass shift of 12 amu confirms that the peak at 528 amu has the (8, 12) stoichiometry of the met-car. Further confirmation was obtained by performing titration experiments in which the $Ti_8C_{12}^+$ cluster was exposed to various polar and nonpolar molecules in the hexapole collision cell ($H_2O$, $NH_3/ND_3$, $C_6H_6$). High-pressure collisions of these molecules resulted in the formation of cluster adducts, e.g., $Ti_8C_{12}^+(ND_3)_n$, in which the molecules preferentially bind to the exposed Ti metal sites.[13] For water and ammonia the most prominent cluster adducts have eight ligands ($n = 8$), while the addition of four ligands ($n = 4$) is most probable for $\pi$-bonded benzene.[13,14] An example mass spectrum of the products of $Ti_8C_{12}^+ + ND_3$ collisions is shown in Figure 3. These results confirm the formation of the $Ti_8C_{12}^+$ met-car and, to our knowledge, represent the first published experimental procedure for its production with magnetron sputtering.

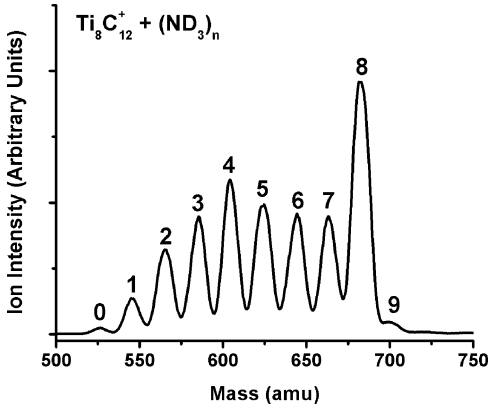


**Figure 3.** Mass spectrum of the products formed from the reaction of $Ti_8C_{12}^+$ with 25% $ND_3$ in He at a collision cell pressure of 12 mTorr.

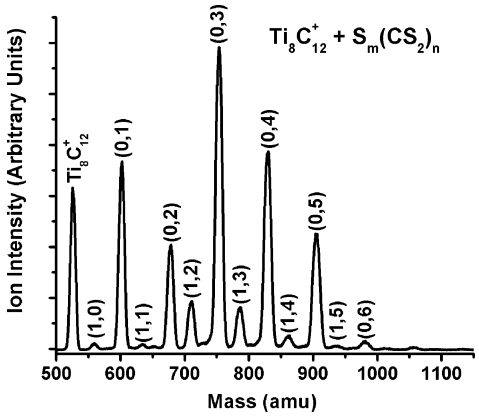


**Figure 4.** Mass spectrum of the products formed from the reaction of $Ti_8C_{12}^+$ with ~1% $CS_2$ in He at a collision cell pressure of 8 mTorr.

**Carbon Disulfide.** The mass spectrum resulting from collisions of $CS_2$ and the $Ti_8C_{12}^+$ met-car is shown in Figure 4. The most intense mass peaks correspond to simple adduct formation, $Ti_8C_{12}^+(CS_2)_n$, with $n = 3$ being the most prominent peak and no detectable products for $n > 6$. Smaller peaks are also observed whose masses correspond to reaction products in which one molecule of $CS_2$ dissociates to leave a sulfur atom on the met-car cluster and other $CS_2$ molecules bind either intact or dissociatively. The overall reaction leading to the observed products can be written as

$$Ti_8C_{12}^+ + (m+n)CS_2 \rightarrow (Ti_8C_{12}^+)S_m(CS_2)_n + mCS_{(g)} \quad (1)$$

with $m = 0$ corresponding to simple adduct formation and $m = 1$ representing products in which one $CS_2$ molecule has dissociated. In this paper, we will use the notation $(m, n)$ to refer to specific products, with $(m = 0, n)$ peaks referred to as "adducts" and the $(m \geq 1, n)$ peaks as "reaction products". The most intense peaks for both series of products have only a few $CS_2$ molecules bonded to the cluster, i.e., $(0, n = 3-4)$ and $(1, n = 2, 3)$. The peak intensities of the reaction products $(1, n = 0, 1, 5-7)$ are very small, and no adducts or reaction products could be detected for $n > 7$. Raising the pressure of the $CS_2$/He collision gas did not increase the intensity of species at higher mass, but instead attenuated the intensity of the entire spectrum. Lowering the pressure of the collision gas shifts the intensity distribution to lighter species, including the bare met-car cluster. These observations suggest that the intensity distribution of the mass spectrum in Figure 4 is representative of the relative

formation probabilities for the various adduct and reaction products with $CS_2$.

As noted previously, the probability of adduct formation between the $Ti_8C_{12}^+$ met-car and polar molecules such as $H_2O$ and $NH_3$ is a maximum at $n = 8$, which is consistent with one molecule bound to each of the eight exposed Ti atom sites.[8,9,13] Aromatic molecules such as $C_6H_6$ preferentially form $\pi$-bonds to the four "outer" Ti atoms of the met-car cluster, and adducts with $n = 4$ are the most prominent.[8,13] Adduct formation with $CS_2$ does not conform to either case, but instead shows a significant intensity drop off for clusters with $n > 5$ and a maximum at (0, 3) (see Figure 4).

These observations may provide insight on how $CS_2$ binds to the met-car cluster. In the condensed phase, $CS_2$ is known to form complexes with metal centers via a head-on coordination with one sulfur atom, side-on coordination with one sulfur and a carbon, and bridging coordination between two or three metal atoms.[30,31] With a combination of these binding configurations, it would be possible to fill all eight Ti atom sites of the met-car with only five $CS_2$ molecules, i.e., two $CS_2$ molecules bonded to one Ti atom each, and three $CS_2$ molecules bridge-bonded to two Ti atoms.

To investigate the relative stability of various types of bonding, we performed density functional (DFT) calculations for one $CS_2$ molecule bonded to the $Ti_8C_{12}^+$ met-car cation. Calculations were carried out with all-electron DFT with the DMol$^3$ code found within the Materials Studio modeling package (Accelrys Inc.).[32,33] A double numerical basis set with p- and d-polarization functions comparable in accuracy to a Gaussian 6-31G* basis was used. The generalized gradient approximation (GGA), with the revised version of the Perdew−Burke−Ernzerhof (RPBE) functional, is used here, which gives the best description of the experimental observed frequency spectra for $Ti_8C_{12}$.[9,34] Previous studies with the RPBE functional show absolute errors of less than 0.25 eV for the bonding energies of CO, $SO_2$, $H_2O$, and $NH_3$ on titanium carbide systems.[9,35] The starting geometry for the $Ti_8C_{12}^+$ met-car cation was calculated by using the same level of code starting with the structure for neutral $Ti_8C_{12}$ taken from previous studies.[10] Calculations show the $Ti_8C_{12}^+$ adopts a tetrahedral $T_d$-like ($C_1$) asymmetric structure with a doublet as the ground state. No symmetry constraints are imposed, allowing the $Ti_8C_{12}^+$ cluster to relax in response to binding of the $CS_2$ molecule. Transition states here were identified by using the combination of synchronous transit methods and eigenvector following, and verified by the presence of a single imaginary frequency from a sequential vibrational frequency analysis.[36,37]

Calculations for several initial $CS_2$ geometries were performed: (1) $Ti^{(i)}-SCS-Ti^{(o)}$ bridge-bonding geometry involving an inner and outer Ti atom; (2) $Ti^{(i,o)}-SCS$ bonding on both inner and outer Ti atoms; and (3) $Ti^{(i,o)}-CS_2$ bonding on both inner and outer Ti atoms. The calculations show that the bridge-bonded $Ti^{(i)}-SCS-Ti^{(o)}$ configuration lies ~1.4 eV lower in energy than the separated met-car cluster and $CS_2$ molecule, and is more stable than the single-bonded $Ti^{(i,o)}-SCS$ configurations by at least 0.8 eV (structures I−III in Figure 5). Calculations with initial $Ti^{(i,o)}-CS_2$ structures are found to be unstable and geometry optimization moves the $CS_2$ molecule to the bridge-bonded site. As shown in Figure 5, the calculated bridge-bonded structure III results in an "adsorbed" $CS_2$ molecule that is bent, with the center C-atom bonded to one of the met-car C-atoms adjacent to the outer $Ti^{(o)}$ site. Binding of the $CS_2$ molecule in this configuration also strongly distorts the met-car structure.

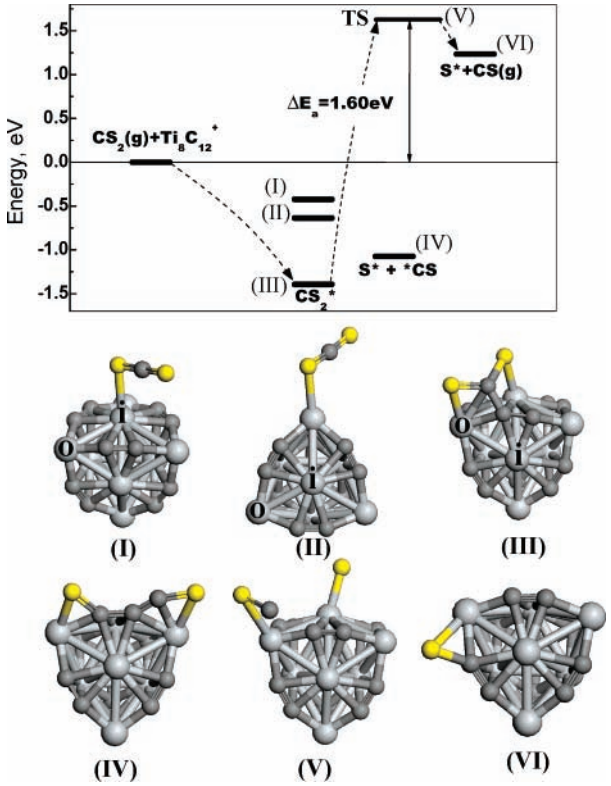


**Figure 5.** Calculated energy diagram (top panel) and the corresponding structures I−VI (lower panel) for the adsorption of $CS_2$ on the $Ti_8C_{12}^+$ met-car. The energies in the top panel are expressed with respect to the free $Ti_8C_{12}^+$ cluster and $CS_2$ molecule in the gas phase. In the lower panel, light gray atoms = titanium (Ti atoms labled "o" represent $Ti^{(o)}$ sites, while those labled "i" represent $Ti^{(i)}$ sites), dark gray = carbon, and yellow = sulfur. The dotted line in the energy diagram is used to guide the reader through the reaction coordinate.

Assuming bridge-bonded $CS_2$ is preferred over the single-bonded configurations, it is possible to speculate on the structures of the more prominent $Ti_8C_{12}^+(CS_2)_n$ adducts observed in the mass spectrum (Figure 4). Specifically, the most intense (0, 3) adduct peak could have three bridge-bonded $CS_2$ molecules leaving one open bridge site, or one open $Ti^{(i)}$ atom and one open $Ti^{(o)}$ atom on opposite sides of the met-car cluster. It follows that the (0, 4) adduct would have four bridge-bonded $CS_2$ molecules with all the Ti atoms involved in adduct binding, but its formation may be slightly less favorable than (0, 3) for steric reasons. The (0, 5) adduct may be a result of three bridge-bonded and two less stable single-bonded configurations, involving the $Ti^{(i)}-SCS$ (I) and $Ti^{(o)}-SCS$ (II) structures; this adduct would also occupy all eight Ti metal sites. The fact that the (0, 6) adduct is very weak in the mass spectrum (see Figure 4) suggests that adding another $CS_2$ molecule to (0, 5) results in considerable crowding and the unfavorable replacement of one bridge-bonded $CS_2$ with two, less stable single-bonded $CS_2$ molecules.

There are, of course, other possible structures for the prominent mass peaks in Figure 4 including the reaction product resulting from the dissociation of $CS_2$ in which both the S-atom and CS fragment remain on the met-car cluster. For example, the (0, 3) adduct peak could result from the addition of two intact $CS_2$ molecules and one $CS_2$ molecule that dissociates into CS and S fragments that occupy two Ti atom sites. This cluster product would have a minimum of four Ti atoms bonded depending on the orientation of the adsorbed $CS_2$ molecules. The plausibility of such products was investigated by calculating the binding energy of an S-atom and CS fragment on the met-

car cation. A number of single- and bridge-bonded configurations are possible, with the two fragments bound at different points on the met-car surface. The lowest energy structure found in this work has the S-atom and the CS fragment bridge-bonded in a $Ti^{(o)}-S-CC-CS-Ti^{(o)}$ configuration along one edge of the met-car cluster (structure IV in Figure 5). The calculated total energy is only 0.4 eV higher than the bridge-bonded, intact $CS_2$ adduct III, and more stable than the either the single-bonded Ti−SCS or structures I and II. Structures III and IV also highlight the fact that the carbon atoms of the met-car cluster play a key role in determining its ability to bind and react with small molecules.

Direct evidence for the dissociation of $CS_2$ comes from the observation of product masses corresponding to $Ti_8C_{12}^+S(CS_2)_n$ species in which one $CS_2$ molecule dissociates to leave an S-atom while the CS fragment is presumably lost to the gas phase. DFT calculations show that the energetically favored structure of the met-car with one S-atom attached is a bridge-bonded $Ti^{(o)}-S-C$ configuration (structure VI in Figure 5). The calculated total energy of the products, $Ti_8C_{12}^+(S)$ plus a free CS molecule, however, lies 1.23 eV higher in energy than the initial reactants. The transition state (structure V in Figure 5) is predicted to lie at even higher energy, with a minimum barrier of +1.6 eV. The latter reflects the relatively strong C−S bond in $CS_2$ (4.46 eV).[31] The small intensity of the mass peak assigned to the $Ti_8C_{12}^+(S)$ reaction product (see Figure 4) is consistent with an endothermic process; however, its presence suggests that there is some probability for this reaction under our experimental conditions. Mass spectra presented in this work were taken with the hexapole ion guide kept at ground potential, so that the relative ion−molecule collision energies mirrored the kinetic energy distribution of the incoming $Ti_8C_{12}^+$ ions (≤1 eV in the lab frame). This relative collision energy could be used to surmount the barrier for dissociation, but we were not able to confirm this hypothesis as attempts to raise the collision energy resulted in signal levels that were too low to make meaningful intensity measurements.

We note that the peak intensities for the reaction products dramatically increase from (1, $n = 0$, 1) to (1, $n = 2$, 3) (see Figure 4). This trend suggests that the addition of one or more $CS_2$ molecules increases the probability for the dissociation reaction, either by lowering the barrier or stabilizing the product cluster, or both. Moreover, the peak intensities of the reaction products (1, $n = 0-5$) roughly follow the intensities of the adduct peaks ($m = 1-6$, 0), suggesting that the reaction products result from the formation of a cluster adduct on which one $CS_2$ molecule dissociates. For example, the $(Ti_8C_{12}^+)S(CS_2)$ reaction product could be formed by the addition and dissociation of a $CS_2$ molecule onto the $(Ti_8C_{12}^+)(CS_2)$ cluster adduct, rather than simple association of an intact $CS_2$ molecule onto the $(Ti_8C_{12}^+)S$ reaction product. The latter process would appear unlikely given the very small probability for forming the $(Ti_8C_{12}^+)S$ reaction product (see Figure 4). Hence, we can write the formation of the association and reaction products as alternative reaction paths for the sequential addition of $CS_2$ molecules, i.e.,

$$Ti_8C_{12}^+(CS_2)_{n-1} + CS_2 \rightarrow Ti_8C_{12}^+(CS_2)_n \qquad (2a)$$

$$Ti_8C_{12}^+(CS_2)_{n-1} + CS_2 \rightarrow (Ti_8C_{12}^+)S(CS_2)_{n-1} + CS_{(g)} \qquad (2b)$$

with n ≥ 1. Although the current experiments do not provide conclusive evidence for the mechanism given by reaction 2, it is nonetheless useful to consider alternative pathways as they address the possibility of modifying the reactivity of the met-car by the adsorption of a few molecules.[38]

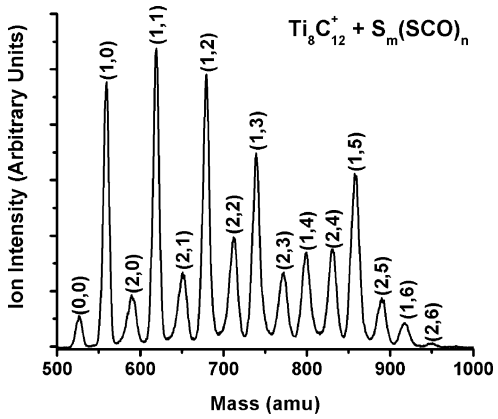


**Figure 6.** Mass spectrum of the products formed from the reaction of $Ti_8C_{12}^+$ with ~1% SCO in He at a collision cell pressure of 8 mTorr.

Changes in reactivity induced by molecular adsorption are most likely a result of charge transfer between the adsorbate and the met-car that modifies the electron distribution (effective oxidation state) at the unoccupied Ti metal sites. Our calculations confirm this and also reveal a dependence on the net transfer of electron density with the bonding configuration. Specifically, a Mulliken population analysis was carried out to estimate the partial charge on each atom and to investigate qualitative trends in charge redistribution for each bonding configuration. For the single-bonded $Ti^{(i)}-SCS$ and $Ti^{(o)}-SCS$ configurations (structures I and II in Figure 5), the calculations show little or no transfer of electron density between the $CS_2$ molecule and the met-car cation. On the other hand, the bridge-bonded $Ti^{(o)}-SCS-Ti^{(i)}$ configuration (structure III in Figure 5) leads to a significant transfer of electron density (0.36e) from the met-car to the $CS_2$ molecule. This is accompanied by an overall decrease in electron density throughout the met-car, most notably at other outer $Ti^{(o)}$ atom sites and the $C_2^-$ units. This reduction in electron density, while the opposite of what is observed for electron donating species such as thiophene,[38] leads to a decrease in effective coordination number and an increase in reactivity.[25] The ability to donate and accept electronic charge depending on whether the adsorbate is nucleophilic (e.g., $H_2O$, $NH_3$, $C_6H_6$) or strongly electron withdrawing (e.g., Cl, I), respectively, is a general feature of molecular binding to the met-car clusters.[9,10,25,39] This characteristic of the met-car cluster makes it particularly versatile for reaction studies as a catalytic "nanoparticle".

By way of comparison, only a few published studies have examined the reaction of $CS_2$ with metal-containing clusters in the gas phase. Most of the published work focuses on gas-phase reactions of single transition metal cations $M^+$ (M ≡ V, Mo, Sc, and Ti) where the two main products are $MS^+$ and $MCS^+$.[40−42] A set of papers by Koszinouski et al. investigated the reactions of $Fe_n^+$ ($n = 1-6$) clusters with $CS_2$ and COS using a guided-ion beam technique and Fourier transform ion cyclotron resonance mass spectrometry.[43,44] They find that the main products of $Fe_n^+ + xCS_2$ at low collision energies (≤1 eV) are the formation of $Fe_nS^+$ and $Fe_{n-1}(CS_2)_x$, where $CS_2$ is found to substitute for an Fe atom in direct association. The formation of metal−sulfur products through the loss of the CS radical is consistent with the observations presented here (see Figure 4).

**Carbonyl Sulfide.** The mass spectrum in Figure 6 shows that the interaction of carbonyl sulfide (SCO) with $Ti_8C_{12}^+$ does not result in association adducts, but instead leads to two sets of reaction products involving sulfur transfer. The overall stoichi-

ometry of the observed reactions with SCO can be written as

$$Ti_8C_{12}^{+} + (m+n)(SCO)_{(g)} \rightarrow (Ti_8C_{12}^{+})S_m(SCO)_n + mCO_{(g)} \quad (3)$$

with $m = 1$ and 2 corresponding to the dissociation of one or two SCO molecules, respectively. The most prominent mass peaks are for the dissociation of one SCO molecule ($m = 1$, $n$) and the series exhibits significant intensity drops at $n = 4$ and 6, with no detectable products at $n > 6$. For the dissociation of two SCO molecules ($m = 2$, $n$), the intensity distribution of the product peaks is similar in that there exist two intensity drops, albeit shifted to $n = 3$ and 5, and there are no discernible products for $n > 6$. Variations in the pressure of the SCO/He collision gas mix did not significantly alter the relative peak intensities across the entire mass spectrum.

The observation of a sudden decrease in the peak intensities for both product series after the (1, 3) and (2, 2) peaks can be rationalized as ligand binding on the four outer $Ti^{(o)}$ atoms on the met-car via a combination of sulfur atoms and SCO molecules. From theoretical calculations on other ligands such as $H_2O$ and CO, the outer $Ti^{(o)}$-atoms are expected to be the most reactive and thus are expected to bind ligands first.[9,16] The origin of the second set of intensity drops at (1, 6) and (2, 5) is less obvious as binding to all Ti atoms would require a total of eight ligands. This suggests that some of the SCO molecules are bound to the met-car in a way as to take up more than one Ti site, similar to the bridge-bonding configuration discussed in the previous section for $CS_2$. Alternatively, the SCO molecule dissociates on the met-car with the S-atom and CO products binding two Ti sites. The high stability of the CO molecule and the relatively weak $Ti^{(i,o)}$−CO association bond,[9,10] however, would argue against the CO fragment remaining on the cluster, especially if there is excess energy released into the product cluster as a result of reaction. Without substantial collisional cooling in the gas cell, it is likely that the CO fragment is released into the gas phase with some excess energy.

As noted above, the majority of the products detected contain one or two S-atoms and intact SCO molecules. As in the case of $CS_2$, the intact SCO molecules can bind to the met-car via end-on or side-on to a single Ti site, or through bridge-bonding between two Ti-atoms. In addition, dissociation of an SCO molecule on the met-car where both the S-atom and CO fragment remain bound would be indistinguishable from an intact SCO in our experiment and is also considered. The relative stabilities of these different SCO binding configurations were calculated with DFT as described in the previous section for $CS_2$. The calculated structures and relative energies are shown in Figure 7. For a single SCO molecule, a bridge-bonded structure III is found to be the lowest energy configuration compared with end-on Ti−SCO configurations (I and II) and the dissociation product in which the S-atom and CO molecule remain bound to the met-car (IV). The bridge-bonded structure III is analogous to that found for the $CS_2$ molecule, in which the S-atom is bound to an inner $Ti^{(i)}$−atom, the O-atom is bound an outer $Ti^{(o)}$-atom and the C-atom is bound to a met-car C-atom of the adjacent $C_2$ unit. The end-on Ti−SCO binding configurations are also similar to those calculated for $CS_2$, as are the binding sites on the met-car for the S-atom and the molecular fragment resulting from dissociative adsorption. For the latter, the S-atom is bridge-bonded in a $Ti^{(o)}$−S−C configuration for both SCO and $CS_2$ (structure IV in Figures 5 and 7), whereas the CO fragment from SCO is bound only to a $Ti^{(o)}$ atom while the CS fragment from $CS_2$ is predicted to be bridge-bonded.

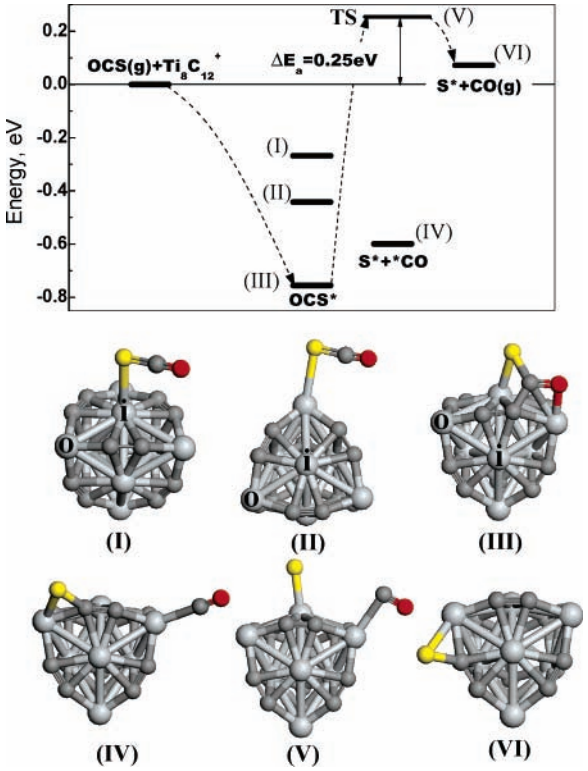


**Figure 7.** Calculated energy diagram (top panel) and the corresponding structures I−VI (lower panel) for the adsorption of SCO on the $Ti_8C_{12}^{+}$ met-car. The energies in the top panel are expressed with respect to the free $Ti_8C_{12}^{+}$ cluster and SCO molecule in the gas phase. In the lower panel, light gray atoms = titanium (Ti atoms labled "o" represent $Ti^{(o)}$ sites, while those labled "i" represent $Ti^{(i)}$ sites), dark gray = carbon, red = oxygen, and yellow = sulfur. The dotted line in the energy diagram is used to guide the reader through the reaction coordinate.

DFT calculations were also used to investigate the energetics and structures involved in the dissociation reaction between SCO and the met-car leading to a S-atom bound to the met-car and a free CO molecule. The calculated energy of the dissociation products, $Ti_8C_{12}^{+}(S) + CO$, is almost thermoneutral relative to that of the reactants (+0.06 eV; see VI in Figure 7), with a substantially lower transition state barrier (+0.25 eV; see V in Figure 7) than in the case of $CS_2$. The C−S bond is significantly weaker in SCO (3.12 eV) than in $CS_2$ (4.46 eV) and this is reflected in the relative energies of the products and barriers for the dissociation reaction.[31] The latter are especially evident in the experimental mass spectra where the mass peak associated with the $Ti_8C_{12}^{+}(S)$ reaction product is very prominent in the product spectrum for reaction with SCO (Figure 6), whereas it appears as a minor peak in the product spectrum for $CS_2$ (Figure 4).

In general, the product mass spectrum from reaction with SCO shows that all products can be associated with dissociation reactions leading to one ($m = 1$) or two ($m = 2$) sulfur adatoms on the met-car cluster (see reaction 3). The mechanistic question arises as to whether the two series of peaks represent independent pathways or share common precursors, as in the case of reactions 2a and 2b for $CS_2$. For SCO, however, there is no evidence of simple association, so that the possible mechanisms only involve the combination and relative order of dissociation and intact molecule addition steps. For the reaction series resulting in one sulfur adatom ($m = 1$ in reaction 3), the first peak corresponding to $(Ti_8C_{12}^{+})S$ is one of the most intense peaks in the experimental spectrum (see Figure 6). This observation would argue for a mechanism in which the first

SCO molecule interacting with the bare met-car cluster results in dissociation and sulfur atom binding, followed by subsequent addition of intact SCO molecules to form the ($m = 1$, $n$) series of products, i.e.,

$$Ti_8C_{12}^{+} + SCO_{(g)} \rightarrow (Ti_8C_{12}^{+})S + CO_{(g)} \quad (4a)$$

$$(Ti_8C_{12}^{+})S + n(SCO)_{(g)} \rightarrow (Ti_8C_{12}^{+})S(SCO)_n \quad (4b)$$

The intensity pattern for the second series of mass peaks leading to two sulfur adatoms, ($m = 2$, $n$), appears to increase as the first series of peaks, ($m = 1$, $n$), decreases in intensity. While this may suggest they are related, several mechanisms involving the order of adduct addition and dissociation of two SCO molecules are possible. As noted earlier, identification of the reaction pathway is only relevant to how the electronic structure of the met-car cluster changes with the addition of strongly bounded sulfur atoms and SCO molecules and how this influences its ability to undergo further reaction. Our calculations show that SCO behaves much like $CS_2$ in the way it affects the electron density of the met-car. Similar to the case of $CS_2$ binding, the single-bonded $Ti^{(o)}-SCO$ and $Ti^{(i)}-SCO$ configurations lead to small increases in the electron density of the met-car (+0.14e and +0.11e, respectively), while the bridge-bonded $Ti^{(o)}-SCO-Ti^{(i)}$ configuration results in significant charge transfer from the met-car (−0.38e) to the SCO molecule. This in turn modifies the other Ti atoms sites and $C_2^-$ units. The effect of such charge transfer on the met-car reactivity is currently the subject of a more extensive computational study involving the interaction of the $Ti_8C_{12}^+$ cluster with as many as eight SCO molecules.

As mentioned in the previous section, there are only a limited number of studies on the reaction of metal clusters with $CS_2$ and SCO in the gas phase. The photochemistry of SCO adsorbed onto $Ag_n$ ($n \geq 9$) clusters is found to exhibit an even−odd dependence. The odd numbered $Ag_nSCO^+$ clusters ($n \geq 9$) undergo sulfur transfer via photodissociation into $Ag_nS^+$ while the even numbered clusters do not exhibit sulfur transfer.[45] In another study, $Fe_n^+$ ($n = 2-6$) clusters are found to afford multiple S-atom transfer in the reaction with SCO.[43,44] The authors do not comment on the formation of association or mixed reaction/association products. While not directly related to metal compound clusters, such as the met-car, these studies show the main reaction pathway for metal cluster reactions with SCO is via S-atom transfer.

**Sulfur Dioxide.** The mass spectrum of the products (300−1000 amu) resulting from $Ti_8C_{12}^+ + SO_2$ collisions is shown in Figure 8a. The bare $Ti_8C_{12}^+$ cluster and the $Ti_8C_{12}^+(SO_2)$ adduct are the most prominent peaks with a number a smaller mass peaks lying between them. In addition, there are many smaller peaks lying above and below this mass range indicative of extensive reaction pathways for $SO_2$. In particular, the product mass peaks observed at masses lower than the bare met-car must result from reactions that lead to decomposition of the met-car cluster itself. For the purposes of this work, we will focus on the more intense product peaks that appear between the bare met-car and the $SO_2$ adduct as shown in the highlighted region of Figure 8a and on an expanded scale in Figure 8b. Further analysis of the higher and lower mass products will be discussed in a future publication.

The two-to-one mass coincidence of oxygen-16 to sulfur-32 requires the use of isotopically enriched samples to determine the precise stoichiometry of the individual mass peaks. By comparing the relative mass shift of each peak with "normal"

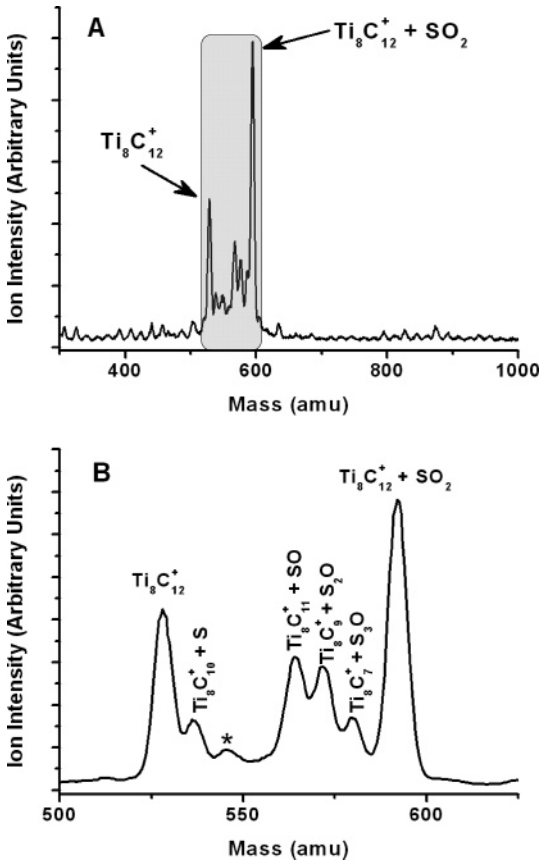


**Figure 8.** (a) Mass spectrum of the products formed from the reaction of $Ti_8C_{12}^+$ with ~10 mTorr of neat $S^{34}O_2$. (b) Expanded view of the mass spectrum between 500 and 600 amu from Figure 8a.

$SO_2$, carbon-13 labeled $Ti_8C_{12}^+$, and $SO_2$ enriched with sulfur-34 or oxygen-18, we were able to assign the products as shown in Figure 8b. From this analysis we find two types of reaction products that result in the loss of carbon atoms from the met-car: one with complete oxygen removal and the others with one SO fragment remaining. The products can be described by the following reaction:

$$Ti_8C_{12} + ySO_{2(g)} \rightarrow Ti_8C_{(12-x)}S_yO_{(2y-x)} + x(CO)_{(g)} \quad (5)$$

where $x = 1-3$, 5 and $y = 1-3$. The most abundant reaction product is $Ti_8C_{11}^+(SO)$ ($x = y = 1$) followed by $Ti_8C_9^+(S_2O)$ ($x = 3$, $y = 2$). The peak labeled with an asterisk could not be assigned to reaction 5 or other possible products involving $SO_2$.

In all three molecules studied, $CS_2$, SCO, and $SO_2$, dissociation reactions on the met-car lead to sulfur atoms (or fragments) that remain bound to the met-car cluster. For $CS_2$ and SCO, the dissociation also involves the loss of a stable diatomic molecule, CS and CO, respectively, that presumably goes into the gas phase and helps carry away excess energy of reaction. In the dissociation of $SO_2$, sulfur can be bound to the met-car as an atom or a SO fragment along with one or two oxygen atoms that react with the carbon atoms of the met-car structure to form CO, rather than combine and "desorb" as molecular oxygen. In this respect, the reaction/dissociation of $SO_2$ with the met-car is similar to that of $O_2$, as the latter results in extensive decomposition of the met-car cluster including the formation of CO.[5] The sequence of observed products, $Ti_8C_{11}^+(SO)$, $Ti_8C_9^+(S_2O)$, and $Ti_8C_7^+(S_3O)$, also suggests that the first $SO_2$ molecule can dissociate to form a bound SO group and one CO molecule, but subsequent addition and reaction

leads to binding of a sulfur atom and the loss of both oxygen atoms by CO formation.

Recent X-ray absorption and photoemission experiments show that $SO_2$ dissociates to sulfur and oxygen adatoms on bulk TiC and MoC.[46,47] The authors report observing the formation of $SO_3$ and $SO_4$ species by way of photoemission spectra; however, they did not report any evidence for SO species on the surface or for gas-phase CO formation in thermal desorption experiments. On the other hand, SO has been detected on Pt, Pd, and Cu metal surfaces as a product of $SO_2$ decomposition.[48] In addition, SO is known to act as a ligand with transition metal complexes in condensed phase inorganic chemistry. Therefore, it is possible the SO fragment remains intact.

In a study directly related to the work reported here, Liu et al. used DFT to investigate the reactivity of $SO_2$ with the neutral $Ti_8C_{12}$ met-car. They predict that $SO_2$ bonds via a $\eta$-3 configuration, with the sulfur bound to one inner $Ti^{(i)}$ atom and the oxygen to two outer $Ti^{(o)}$ atoms. In this configuration, the molecule is predicted to spontaneously dissociate into S and O adatoms. The sulfur atom remains bound to an inner titanium atom while the oxygen atoms form a bridging bond between the outer titanium and carbon atoms. These calculated results would suggest the SO unit does not stay intact. Furthermore, the reported final configuration appears to be a probable transition state to the products we observe experimentally. While Liu et al. did not calculate the barrier for the loss of CO, it is plausible that after dissociation and migration to the bridging site, enough energy could remain to overcome such a barrier. It should be noted that the calculations reported by Liu and co-workers were done on neutral species while the work here was done with cations. The difference in electronic structure could play an important role in this process. Overall, the experimental results support the calculated reaction mechanism for $SO_2$ on the $Ti_8C_{12}$ met-car and currently calculations are underway to determine the barrier for CO loss from the cation.

## IV. Summary

Using a newly developed cluster beam machine, a series of gas-phase $Ti_xC_y^+$ clusters ($x/y$ = 3/5, 4/7, 5/9, 6/9, 7/12, 8/12, 9/12) were generated by reactive sputtering in a magnetron cluster source. The most prominent cluster in the mass spectrum was determined to be the $Ti_8C_{12}^+$ met-car cation by way of carbon-13 substitution and association reactions with simple molecules with use of a gas collision cell. The reactivity of the size-selected $Ti_8C_{12}^+$ met-car with triatomic sulfur compounds, $CS_2$, SCO, and $SO_2$, was investigated and the resulting product mass spectra indicate an increase in activity as the oxygen-to-sulfur ratio increases ($SO_2$ > SCO > $CS_2$). The observed products range from almost pure association for $CS_2$, sulfur transfer and association for SCO, to sulfur and oxygen transfer along with decomposition of the met-car cluster through the loss of carbon (presumably in the form of CO) for $SO_2$.

Density functional theory was employed to investigate possible configurations of single molecule−cluster bonding (head-on and bridging) along with barriers to formation of the first set of dissociation products observed in the mass spectra. Calculations indicate that bridge bonding is energetically preferred for the intact $CS_2$ and SCO molecules and for deposited sulfur atoms that result from dissociation. These bridge-bonded configurations involve direct bonding to carbon atoms of the met-car cluster, and underscore the important role that the carbon atoms play in the electronic structure and reactivity of the met-car cluster. The calculated barrier for $CS_2$ dissociation on the metcar is significantly higher than that for SCO, in qualitative agreement with the relative yields of dissociation products observed in the experimental mass spectra and the relative gas-phase C−S bond strengths. Following the trend of increasing reactivity with oxygen content, $SO_2$ interactions with the met-car lead to multiple sulfur transfer (up to 3 S-atoms) and decomposition of the met-car cluster through the loss of carbon atoms, presumably through CO formation. The calculations presented here were limited to the interaction of a single molecule and the $Ti_8C_{12}^+$ met-car cluster, and a more comprehensive DFT study involving multiple ligands is currently in progress.

**Acknowledgment.** The authors wish to thank Dr. Scott Anderson, University of Utah, for guidance on instrumentation design and James Muckerman, Brookhaven National Laboratory, for helpful discussions. We also wish to thank Dr. Robert J. Beuhler, Fred Maier, and Eugene Von Achen, Brookhaven National Lab, and Andy Jacobs, SUNY Stony Brook, for their contributions to the development and construction of the instrument. This research was carried out at Brookhaven National Laboratory under contract DE-AC02-98CH10086 with the U.S. Department of Energy (Division of Chemical Sciences).

## References and Notes

(1) Guo, B. C.; Kerns, K. P.; Castleman, A. W., Jr. *Science* **1992**, *255*, 1411.
(2) Guo, B. C.; Wei, S.; Purnell, J.; Buzza, S.; Castleman, A. W., Jr. *Science* **1992**, *256*, 515.
(3) Wei, S.; Guo, B. C.; Purnell, J.; Buzza, S.; Castleman, A. W., Jr. *Science* **1992**, *256*, 818.
(4) Wei, S.; Guo, B. C.; Purnell, J.; Buzza, S.; Castleman, A. W., Jr. *J. Phys. Chem.* **1992**, *96*, 4166.
(5) Duncan, M. A. *J. Cluster Sci.* **1997**, *8*, 239 and references therein.
(6) Leskiw, B. D.; Castleman, A. W., Jr. *C. R. Phys.* **2002**, *3*, 251 and references therein.
(7) Dance, I. G. *Chem. Commun.* **1998**, 523.
(8) Rohmer, M.-M.; Benard, M.; Poblet, J.-M. *Chem. Rev.* **2000**, *100*, 495 and references therein.
(9) Liu, P.; Rodriguez, J. A.; Hua, H.; Muckerman, J. T. *J. Chem. Phys.* **2003**, *118*, 7737.
(10) Hou, H.; Muckerman, J. T.; Liu, P.; Rodriguez, J. A. *J. Phys. Chem. A* **2003**, *107*, 9344.
(11) Joswig, J.; Springborg, M.; Siefert, G. *Phys. Chem. Chem. Phys.* **2001**, *3*, 5130.
(12) Dance, I. *J. Chem. Soc., Chem. Commun.* **1992**, 1779.
(13) Guo, B. C.; Kerns, K. P.; Castleman, A. W. *J. Am. Chem. Soc.* **1993**, *115*, 7415.
(14) Deng, H. T.; Kerns, K. P.; Castleman, A. W. *J. Am. Chem. Soc.* **1996**, *118*, 446.
(15) Auberry, K. J.; Byun, Y. G.; Jacobson, D. B.; Freiser, B. S. *J. Phys. Chem. A* **1999**, *103*, 9029.
(16) Poblet, J.-M.; Bo, C.; Rohmer, M. M.; Bernard, M. *Chem. Phys. Lett.* **1996**, *260*, 577.
(17) Hwu, H. H.; Chen, J. G. *Chem. Rev.* **2005**, *105*, 185.
(18) Oyama, S. T. Introduction to the Chemistry of Transition Metal Carbides and Nitrides. In *The Chemistry of Transition Metal Carbides and Nitrides*; Oyama, S. T., Ed.; Blackie Academic and Professional: Glasgow, Scotland, 1996; pp 1 and references therein.
(19) Chen, J. G. *Chem. Rev.* **1996**, *96*, 1477.
(20) Levy, R. L.; Boudart, M. *Science* **1973**, *181*, 547.
(21) Oyama, S. T. *Catal. Today* **1992**, *15*, 179.
(22) Hwu, H. H.; Fruhberger, B.; Chen, J. G. *J. Catal.* **2004**, *221*, 170.
(23) Fruhberger, B.; Chen, J. G.; J. Eng, J.; Bent, B. E. *J. Vac. Sci. Technol. A* **1996**, *14*, 1475.
(24) Hwu, H. H.; Chen, J. G. *Surf. Sci.* **2004**, *557*, 144.
(25) Liu, P.; Rodriguez, J. A. *J. Chem. Phys.* **2003**, *119*, 10895.
(26) Deng, H. T.; Guo, B. C.; Kerns, K. P.; Castleman, A. W. *J. Phys. Chem.* **1994**, *98*, 13373.
(27) Deng, H. T.; Kerns, K. P.; Bell, R. C.; Castleman, A. W. *Int. J. Mass Spectrom. Ion Proc.* **1997**, *167/168*, 615.
(28) Jones, R. M.; Anderson, S. L. *Rev. Sci. Instrum.* **2000**, *71*, 4335.
(29) Hiroki, S.; Sakata, K.; Sugiyama, N.; Muramoto, S.; Abe, T.; Murakami, Y. *Vacuum* **1995**, *46*, 681.
(30) Ibers, J. A. *Chem. Soc. Rev.* **1982**, *11*, 57.
(31) Pandey, K. K. *Coord. Chem. Rev.* **1995**, *140*, 37.

(32) Delley, B. *J. Chem. Phys.* **1990**, *92*, 508.
(33) Delley, B. *J. Chem. Phys.* **2000**, *113*, 7756.
(34) Hammer, B.; Hansen, L. B.; Norskov, J. K. *Phys. Rev. B* **1999**, *59*, 7413.
(35) Liu, P.; Rodriguez, J. A.; Muckerman, J. T. *J. Chem. Phys.* **2004**, *121*, 10321.
(36) Baker, J. *J. Comput. Chem.* **1986**, *7*, 385.
(37) Halgren, T. A.; Lipscomb, W. N. *Chem. Phys. Lett.* **1977**, *49*, 225.
(38) Liu, P.; Lightstone, J.; Patterson, M.; Rodriguez, J.; Muckerman, J. T.; White, M. G. To be submitted for publication.
(39) Liu, P.; Rodriguez, J.; Muckerman, J. T. *J. Phys. Chem. B* **2004**, *108*, 18796.
(40) Kretzschmar, I.; Schroder, D.; Schwarz, H.; Rue, C.; Armentrout, P. B. *J. Phys. Chem. A* **2000**, *104*, 5046.
(41) Kretzschmar, I.; Schroder, D.; Schwarz, H.; Armentrout, P. B. *Int. J. Mass Spectrom.* **2003**, *228*, 439.
(42) Kretzschmar, I.; Schroder, D.; Schwarz, H.; Rue, C.; Armentrout, P. B. *J. Phys. Chem. A* **1998**, *102*, 10060.
(43) Koszinowski, K.; Schroder, D.; Schwarz, H. *Eur. J. Inorg. Chem* **2004**, *1*, 44.
(44) Koszinowski, K.; Schroder, D.; Schwarz, H.; Liyanage, R.; Armentrout, P. B. *J. Chem. Phys.* **2002**, *117*, 10039.
(45) Brown, L. A.; Rayner, D. M. *J. Chem. Phys.* **1998**, *109*, 2474.
(46) Rodriguez, J. A.; Dvorak, J.; Jirsak, T. *J. Phys. Chem. B* **2000**, *104*, 11515.
(47) Rodriguez, J. A.; Liu, P.; Dvorak, J.; Jirsak, T.; Gomes, J.; Takahashi, Y.; Nakamura, K. *Surf. Sci. Lett.* **2003**, *543*, L675.
(48) Haase, J. *J. Phys.*: *Condens. Matter* **1997**, *9*, 3647.